Journal of Engineering Physics and Thermophysics, Vol. 73, No. 4, 2000

EXPERIMENTAL STUDY OF FRICTION STRESS ON THE WALL OF A CYLINDRICAL TUBE IN AN OSCILLATING TURBULENT FLOW OF A LIQUID

E. D. Barbashov, B. F. Glikman, and A. A. Kazakov

UDC 532.517.6

Results of experiments where the nonstationary friction stress in an oscillating flow in a cylindrical tube was measured by a mechanical sensor within rather wide ranges of frequency (1–160 Hz) and Reynolds number ($1.7 \cdot 10^4$–$1.2 \cdot 10^5$) are presented. A technique is suggested for calculating dynamic characteristics for the friction stress within three ranges of frequency, for which quasistationary and quasilaminar models of flow and a model for the intermediate frequency range are applicable. On the basis of experimental data, an approximation relation for the transmission ratio of the friction stress as a function of the dimensionless frequency is suggested.

In the case of an oscillating turbulent flow in a tube, two limiting ranges of frequencies exist for which one can rather rigorously use relatively simple mathematical models of liquid flow near the wall and, correspondingly, determine the friction stress on the wall.

One limiting case is low frequencies, for which a quasistationary model of flow is suitable. This possibility is determined by the fact that at low frequencies of oscillations the characteristic time of variation of the parameters of turbulence (the mean period of turbulent pulsations) is much smaller than the period of forced oscillations, and the turbulence is able to change in time with the oscillations of the liquid in the tube.

For smooth tubes we can use here the following relation for the friction stress:

$$\tau_w = \lambda \frac{\rho U^2}{8} \tag{1}$$

and the Blasius relation

$$\lambda = \frac{0.3164}{\mathrm{Re}^{0.25}}. \tag{2}$$

The other limiting case is rather high frequencies, for which the thickness of the laminar sublayer turns out to be larger than the depth of penetration of disturbances from the wall into the flow that are caused by forced oscillations. This is associated with the fact that the thickness of the dynamic layer at the wall in which the velocity changes in the oscillations decreases with increase in the frequency. At certain frequencies this layer becomes comparable to the thickness of the laminar layer and then smaller than it. Here, in a turbulent flow, the variable component of the friction stress on the wall caused by the forced oscillations is described by relations for a laminar flow. We call this mode quasilaminar.

For an oscillating quasilaminar flow the variable component of the friction stress on the wall is determined by the relation [1, 2]

$$\frac{\delta\bar{\tau}_w}{\delta\bar{U}} = \frac{\tau_{w0}\, i^{3/2} J_1 (i^{3/2} R \sqrt{\omega/\nu})}{4U J_2 (i^{3/2} R \sqrt{\omega/\nu})}. \tag{3}$$

"Novotekhnika" Science and Production Association, Moscow, Russia. Translated from Inzhenerno-Fizicheskii Zhurnal, Vol. 73, No. 4, pp. 704-711, July–August, 2000. Original article submitted July 30, 1999.

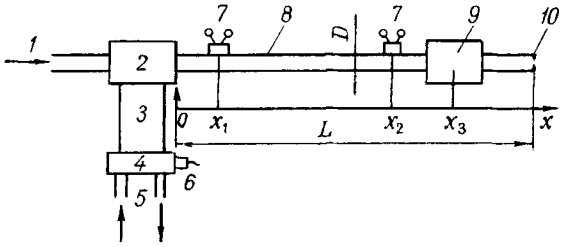

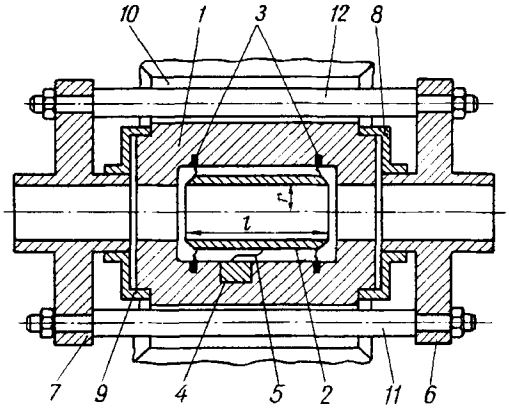

Fig. 1. Schematic of the experimental setup.

Fig. 2. Schematic of the sensor of frictional force.

We note that for the quasilaminar and intermediate regions experimental data on measurement of the friction stress are meager and they do not always confirm the applicability of the quasilaminar model of flow in this region [3, 4].

We measured the friction stress in both the quasistationary and quasilaminar regions and in the region of frequencies between the two limiting cases described above.

The experiments were conducted on the setup whose schematic is presented in Fig. 1. Water was supplied to the flow part of the setup through the tube 1 at a constant mean pressure. Harmonic oscillations of the specified frequency, whose value is determined by the transmission ratio of the reducer 3 and the rotational speed of the hydraulic engine 4, were produced in the system by the pulsator 2. The frequency of the forced oscillations was varied according to a program by assigning the flow rate of oil through the connecting pipes 5 of the hydraulic engine. The rotational speed of the pulsator shaft was registered by a sensor of shaft position 6.

From the pulsator 2 water gets to the studied portion of the cylindrical tube 8 (L = 6.4 m, R = 0.01 m), at whose inlet and outlet pressure pickups 7 were installed, and in front of the outlet throttle orifice 10 a sensor of frictional force*) 9 was mounted.

The sensor of frictional force (Fig. 2) consists of a body 1 and a sensitive element 2 in the form of a thin-walled cylinder (l = 0.05 m, r = 0.01 m), which is attached to the body by elastic elements 3. The immobile part of the inductive displacement sensor 4 is fastened in the body 1, and the mobile part is connected to the sensitive element of the sensor of frictional force 2 by a rod 5. To prevent the introduction of disturbances into the flow the connecting pipes of the flanges 6 and 7 and the channel in the sensitive element 2 are positioned coaxially with the channels in the body 1. To reduce the effect of vibrations of the bench on the sensor of frictional force, the hermetic covers 8 and 9 are made elastic and the body 1 is manufactured with a seismic mass 10 as a single whole. An immobile frame concreted into the base of the setup was used as the seismic mass.

In flow of the liquid through the sensor, the frictional force affects the sensitive element 2, thus causing its displacement (of the order of 10^{-3} mm) and deformation of the elastic elements 3. With the aid of the rod 5 this displacement is transferred to the inductive sensor 4, the signal from which, after amplification, arrives at the recording device.

In the presence of axial vibrations in the systems of the setup, the flanges 6 and 7, which are rigidly connected to each other by rods 11 and 12, can move. However, this does not lead to the appearance of appreciable vibrations of the sensor body 1, which is rigidly connected to the immobile frame concreted into the base of the setup. In the experiments on measuring the variable component of the frictional force, the vibroacceleration did not exceed 0.05 m/sec^2.

*) The authors would like to express their gratitude to P. P. Chelovan', who designed and produced the sensor.

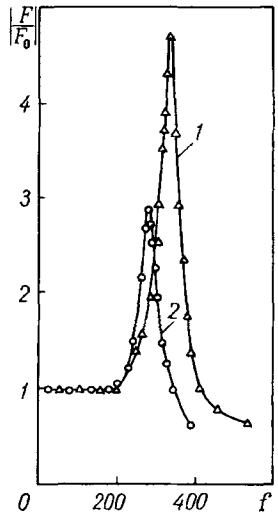

Fig. 3. Dependence of the amplitude of the force measured by the sensor on the frequency of the oscillations: 1) tests of the sensor without a liquid; 2) tests of the sensor filled with water. f, Hz.

To determine the vibration sensitivity, we tested the sensor of frictional force on a vibration table within the range of frequencies of 10–260 Hz at a constant vibroacceleration of 10 m/sec^2. The tests were performed on dry and water-filled sensors. In the range of frequencies up to 160 Hz, in which experiments on measuring the frictional force were conducted, the value of the vibration-induced signal produced by the sensor did not exceed 0.02 N in amplitude. Hence it follows that within the indicated frequency range the signal induced by vibrations of the sensor is expected to be no higher than $0.02 \cdot 0.05/10 = 10^{-4}$ N. Since the amplitude of the forced oscillations of the frictional force measured by the sensor was within the limits to 1 N, the inductions due to vibrations can certainly be neglected.

To determine possible dynamic errors in measuring the friction stress in an oscillating flow, we tested the frequency of the mobile parts of the sensor. The setup included a generator of a harmonic signal, an amplifier, an electromagnet, and an excitation coil mounted directly on the sensitive element 2 (Fig. 2) of the tested sensor. During the frequency tests, the frequency of the excited signal was varied within 1–400 Hz, and the amplitude of the force produced was maintained strictly constant at all excitation frequencies by a special system. Since the excitation coil increased the mass of the mobile parts, i.e., decreased their eigenfrequency of oscillations, the frequency tests of the sensor provided data, with a certain margin, on the frequency range of sensor operation without dynamic distortions.

Figure 3 presents dependences of the ratio of the amplitude of oscillations of the force F measured by the sensor at the given frequency to the amplitude F_0 at the minimum frequency (1 Hz) on the excitation frequency. The tests were conducted with dry (curve 1) and water-filled (curve 2) sensors. The results of the tests showed that the sensitive system of the dry sensor does not give dynamic distortions, i.e., it has a horizontal amplitude-frequency characteristic up to a frequency of 200 Hz and a resonance peak near 335 Hz. For the water-filled sensor, the amplitude-frequency characteristic up to a frequency of 200 Hz virtually did not change, and the resonance was shifted to the region of 275 Hz. Here, the effect of the mass of the added liquid manifested itself in both the sensitive element and the elastic elements of the suspension of the sensitive element. Thus, up to a frequency of 200 Hz the sensor reproduces the frictional force without dynamic distortions.

Static calibrations of the sensor of frictional force were made by two methods: gravimetric and spilling. In the first case, a specified force on the sensitive element was produced by several weights. Here the force was applied in two directions – with and against the stream of the liquid, since it was revealed in the experiments with an oscillating flow that the variable component of the frictional force can exceed its mean value.

The results of the experiments with the weights showed that the calibration characteristic of the sensor is linear and has no hysteresis.

In the other method of calibration, the water flow rate was measured on the setup, the indications of the sensor of frictional force were read, and the pressure drop was measured on the studied section of the tube. The coefficient of resistance λ was calculated from the results of measuring the pressure drop and the flow rate. Comparison with the value calculated by formula (2) showed good agreement, i.e., confirmed the fact that the studied channel is hydraulically smooth. The results of measurement of the frictional force on the sensitive element in spilling coincided with the data of calibration by the gravimetric method.

In the experiments with an oscillating flow the mean pressure at the inlet to the experimental section of the tube was kept constant. The frequency of the oscillations was varied according to a specified cyclogram by controlling the supply of oil to the hydraulic engine of the pulsator.

In the first experiments with the pulsator the signal from the sensor of frictional force was subjected to spectral analysis. It turned out that the spectrum of the signal contains only two substantial components – the frequency of the liquid oscillations produced by the pulsator and the eigenfrequency of the oscillations of the sensitive element. In processing by a narrow-band tracing filter only the fundamental harmonic produced by the pulsator was separated out. The frequency of the eigenoscillations of the sensitive element was suppressed by the filter to the level of noise.

During the experiments, the variable components of the frictional force δF_{fr} and the pressure in front of the sensor of friction $\delta p(x_2)$ (see Fig. 1) and the signal of the pickup of the pulsator position were measured and recorded on a tape recorder. After processing the signals on the tracing filter and a computer, the transfer function $\delta F_{fr}/\delta p(x_2)$ was obtained.

The ratio $\delta F_{fr}/\delta p(x_2)$ is inconvenient for analysis, since it depends on the dynamic properties of the liquid column in the portion of the channel from the pressure pickup to the outlet throttling orifice and on the conditions (impedance) at the tube inlet. Other ratios $\delta F_{fr}/\delta U(x_3)$, $\delta\tau/\delta U(x_3)$, and $\delta\tau/\delta\tau_{qs}$ do not depend on these factors. It should be noted that within the range of frequencies studied, acoustic effects do not influence the readings of the sensor of friction, since the length of acoustic oscillations c/f = 1450/200 = 7.25 m is much larger than the length of the sensitive element of the sensor l = 0.05 m.

The ratio $\delta\tau/\delta\tau_{qs}$ is the most representative, since it characterizes the effects caused by the nonstationarity of the flow in the tube most completely.

The ratios $\delta\tau/\delta\tau_{qs}$ and $\delta F_{fr}/\delta U(x_3)$ are related as follows:

$$\frac{\delta\tau}{\delta\tau_{qs}} = \frac{U}{1.75\pi DL_{s.e}\,\tau_{qs}} \frac{\delta F_{fr}}{\delta U\,(x_3)}, \tag{4}$$

$$\delta\tau_{qs} = 1.75\,\frac{\tau_{qs}}{U}\,\delta U\,(x_3)$$

is the variation of the friction stress in the quasistationary case obtained by linearization of the relationship for the friction stress in a quasistationary turbulent flow

$$\tau_{qs} = \frac{0.3164}{\mathrm{Re}^{0.25}}\,\frac{\rho U^2}{8}.$$

Relation (4) involves the variation $\delta U(x_3)$ not measured in the experiments, and therefore it is necessary to convert from it to the ratio $\delta F_{fr}/\delta p(x_2)$ ($\delta p(x_2)$ is the variation of the pressure in the cross section x_2 of the pressure pickup), which is obtained in the form of primary information in the experiments. This conversion is possible when use is made of the computational ratio $\delta p(x_2)/\delta U(x_3)$, which describes the dynamic characteristics of the liquid column in the tube between the cross sections in which the pressure pickup and the fric-

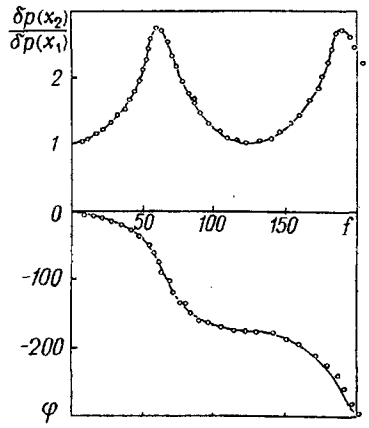

Fig. 4. Ratio $\delta p(x_2)/\delta p(x_1)$ as a function of the frequency of the oscillations (solid curve, calculation; points, experiment). φ, deg.

tion sensor are located (Fig. 1). The ratio $\delta p(x_2)/\delta U(x_3)$ is calculated by a mathematical model of tube flow with account for the boundary condition at the tube end [1-3].

Rather high accuracy of calculations by the mathematical model of flow is confirmed by comparison of the results of the calculations with data of experiments on the setup used. Figure 4 presents experimental points and data of calculations (solid curves) for the dynamic characteristic of the liquid column on the portion of the tube in the form of $\delta p(x_2)/\delta p(x_1)$, where $\delta p(x_1)$ is the variation of the pressure in the cross section x_1 of the pressure pickup at the inlet to the portion of the tube. The calculation results agree well with the experimental data. The magnitude of the second resonance differs slightly from that of the first resonance, which is associated with small friction losses along the length of the channel.

Thus, having introduced the ratio $\delta F_{fr}/\delta p(x_2)$ into Eq. (4), we find an expression for $\delta\tau/\delta\tau_{qs}$ (note that $\delta F_{fr}/\delta p(x_2)$ is a complex quantity) in terms of quantities found experimentally:

$$\frac{\delta\tau}{\delta\tau_{qs}} = \frac{U}{1.75\pi D L_{s.e}\,\tau_{qs}} \frac{\delta p\,(x_2)}{\delta U\,(x_3)} \left|\frac{\delta F_{fr}}{\delta p\,(x_2)}\right| (\cos\varphi_{fr} + i\sin\varphi_{fr}),$$

where $\left|\frac{\delta F_{fr}}{\delta p(x_2)}\right|$ and $(\cos\varphi_{fr} + i\sin\varphi_{fr})$ are the measured values of the modulus and phase of the ratio $\delta F_{fr}/\delta p(x_2)$; $\delta p(x_2)/\delta U(x_3)$ is the transmission ratio of the variations of the pressure in the cross section x_2 and the velocity in the cross section x_3 of the tube, which is calculated by the mathematical model of a nonstationary flow in a tube.

It is shown in [5] that, in studying oscillations in turbulent flows, it is convenient to use the dimensionless "turbulent Stokes number" $\omega_* = \omega D/U_*$ to describe experimental data. The essence of this number is that it is proportional to the ratio of the tube radius to the length of the turbulent diffusion in a period of the oscillations, and it is useful in studying the interaction between imposed forced oscillations and turbulent vortices at a specified Reynolds number. Here the "turbulent Stokes number" ω_* is a measure of the relative distance from the wall up to which nonstationary effects will penetrate into the flow.

Figure 5 presents experimental points for the modulus and the phase φ of the transmission ratio $\delta\tau/\delta\tau_{qs}$ as a function of the parameter ω_*. The same figure gives theoretical curves (solid lines) that consist of three parts. One part (for rather high values of ω_*) is calculated by formula (3) of the quasilaminar model. Another part (for low values of ω_*) is calculated by the quasistationary model, when $\delta\tau/\delta\tau_{qs} = 1$. The third part (for intermediate frequencies ω_*), which lies between the first two, is described by the suggested approximation relation

$$\left|\frac{\delta\tau}{\delta\tau_{qs}}\right| = \frac{\omega_* - 2.5}{1.75}. \qquad (5)$$

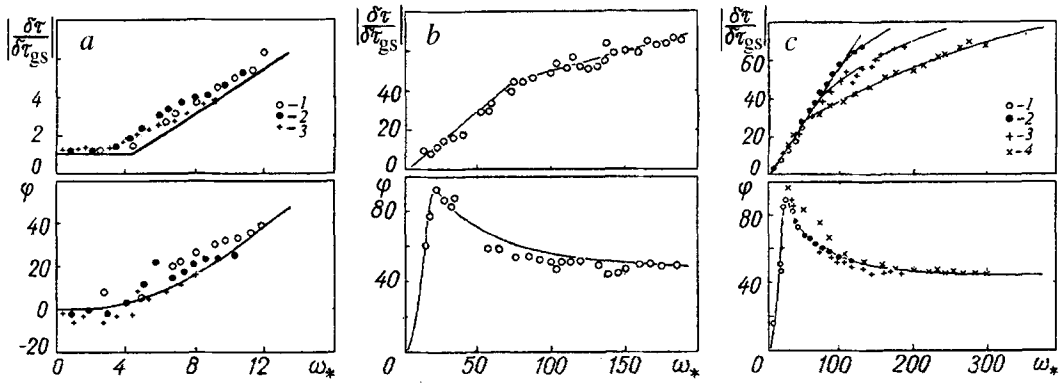

Fig. 5. Ratio $\delta\tau/\delta\tau_{qs}$ as a function of the parameter ω_*: a: 1) Re = $5.9\cdot10^4$; 2) $8.5\cdot10^4$; 3) 10^5; b: Re = $2.4\cdot10^4$; c: 1) Re = $1.1\cdot10^5$; 2) $5.6\cdot10^4$; 3) $2.7\cdot10^4$; 4) $2.5\cdot10^4$.

In construction of the theoretic curves on a computer, the transition from the approximation relation (5) to the curve of the quasilaminar model occurred at the moment when the values of $\left|\frac{\delta\tau}{\delta\tau_{qs}}\right|$ obtained by the approximation relation began to exceed the values obtained by the quasilaminar model.

In the region of small values of the parameter ω_*, smaller than 2.5 (Fig. 5a), the quantity $\left|\frac{\delta\tau}{\delta\tau_{qs}}\right|$ approaches unity, i.e., a quasistationary value. At higher values of the parameter ω_* (Fig. 5b), the experimental points lie on the approximation straight line (5) (solid line). With further increase in the parameter ω_*, the experimental points lie near the theoretic curve for the quasilaminar model (Fig. 5c). All other things being equal, the transition to the quasilaminar model occurs at higher values of ω_* in the case of higher Re numbers.

Studies of the interaction between forced oscillations of a flow and the structure of turbulence in the flow [5] showed that the effect of the nonstationarity on the structure of the turbulence is determined by the interaction between the forced oscillations of the flow and the oscillations corresponding to the characteristic frequencies of the turbulent vortices that carry the main part of the turbulence energy. The dependence for the upper boundary ω_b of the histogram of 95% energy of the turbulent vortices has the form

$$\omega_b = 31\,\mathrm{Re}^{0.125}\left(10^{-(3.32-0.667\log \mathrm{Re})}\right). \tag{6}$$

The values of the frequencies calculated by relation (6) for the experiments whose results are presented in Fig. 5c are as follows: points 1 – ω_b = 139, points 2 – 61, points 3 – 44, points 4 – 30. Analysis of the results of the experiments presented in Fig. 5c indicates that, from both the experimental points and the results of the calculations, the transition from the approximation straight line of formula (5) to the curves of the quasilaminar model of flow occurs at values of ω_* corresponding to about $1.8\omega_b$, where ω_b is calculated by formula (6).

Figure 5 also gives curves and experimental points for the phase-frequency characteristics of the ratio $\delta\tau/\delta\tau_{qs}$, i.e., the phase shift between the variable component of the friction stress on the wall and the variable component of this parameter for the quasistationary case, for which the friction stress is proportional to the mean value of the instantaneous velocity. At low values of ω_* the velocity profile over a period of the oscillations is close to the stationary one [1, 2], and the calculated curves and the experimental points for the phase shift are close to zero, which corresponds to the quasistationary value of the phase shift between the oscillations of the friction stress and the oscillations of the mean velocity.

As ω_* increases, the phase difference between the oscillations of the friction stress and the velocity oscillations (i.e., $\delta\tau_{qs}$) increases to about 90. With further increase in the parameter ω_*, there occurs a transition

to the quasilaminar mode of liquid flow occurs at the wall, in which all variations in the velocity profile in a period of the oscillations occur near the wall in a laminar sublayer and the experimental values of the phase difference tend to the value predicted by the quasilaminar model, 45° [1, 2].

The experimental data on the phase shift φ between the friction-stress oscillations and the velocity oscillations that are presented in Fig. 5 can be approximated by the suggested relation

$$\varphi = \frac{41.4\,(2.5\omega_*)^2}{(2.5\omega_*)^2 - 27\,(2.5\omega_*) + 337},$$

which is shown in the form of solid lines in Fig. 5. It is noteworthy that the curves for the phase shift, in contrast to the curves for the amplitude characteristics, clearly do not stratify respect to the Re number.

NOTATION

τ_w, friction stress on the wall; λ, coefficient of friction resistance; ρ and U, instantaneous values of the density and the mean velocity over the cross section; Re, Reynolds number calculated from U; J_1 and J_2, Bessel functions of the first kind and the first and second order, respectively; $\delta\tau_w$, amplitude of the variation (deviation) of the friction stress on the wall; $\tau_{w0} = u\rho\nu U/R$, friction stress on the wall in a steady-state laminar flow; ν, viscosity of the liquid; R and L, radius and length of the tube; l and r, length and radius of the sensitive element of the sensor; ω, angular frequency of the forced oscillations of the liquid; F, amplitude of the frictional force measured by the sensor; F_0, amplitude of the frictional force measured by the sensor at the minimum frequency of the oscillations (1 Hz); f, frequency of the oscillations; δF_{fr}, variable component of the frictional force; δp, variable component of the liquid pressure; x_1, x_2, and x_3, coordinates (along the tube) of the cross sections where the pressure pickups at the inlet to and the outlet from the tube and the friction sensor are installed; $\delta\tau$, variation of the friction stress measured by the sensor; $\delta\tau_{qs}$, variation of the friction stress calculated for a quasistationary flow; δU, variation of the mean velocity of the liquid in the tube; $L_{s.e}$, length of the sensitive element of the sensor of frictional force; τ_{qs}, mean value of the friction stress in the quasistationary approximation; φ, phase shift between the oscillations of the variable component of the frictional force and the pressure oscillations; $\omega_* = \omega D/U_*$, turbulent Stokes number; D, tube diameter; $U_* = \sqrt{\tau_{qs}/\rho}$, dynamic velocity.

REFERENCES

1. B. F. Glikman, *Mathematical Models of Pneumohydraulic Systems* [in Russian], Moscow (1986).
2. D. N. Popov, *Nonstationary Hydromechanical Processes* [in Russian], Moscow (1982).
3. E. D. Barbashov, B. F. Glikman, A. A. Kazakov, and S. A. Morozov, *Akustich. Zh.*, **42**, No. 3, 478-488 (1996).
4. Zh. X. Mao and T. J. Hanratty, *J. Fluid Mech.*, **170**, 545-564 (1986).
5. S. W. Tu and B. R. Ramparian, *J. Fluid Mech.*, **137**, 31-81 (1983).